California Institute of Technology

W. M. Keck Laboratory of Engineering Materials

DISLOCATION VELOCITY MEASUREMENTS IN COPPER AND ZINC

by

T. Vreeland, Jr.

An extended abstract of a paper to be given at the Seattle-Harrison Colloquium on "Dislocation Dynamics", May 1-6, 1967 sponsored by Battelle Memorial Institute

Submitted to the U. S. Atomic Energy Commission
under Contract # AT(04-3)-473

January 1967

DISLOCATION VELOCITY MEASUREMENTS IN COPPER AND ZINC*

T. Vreeland, Jr.
W. M. Keck Laboratory of Engineering Materials
California Institute of Technology
Pasadena, California

ABSTRACT

Studies of dislocation dynamics in a number of different materials have been reported, but no direct measurements in FCC or HCP metals have appeared in the literature. Studies of slip band growth in the basal system of zinc at this laboratory have indicated that individual dislocations achieve relatively high velocities at the yield stress. This implies that only very short duration loading (μsec) of low dislocation density crystals (<1000 cm^{-2}) will permit direct measurement of the dynamics of motion of individual basal dislocations in zinc. Suitable single crystal specimens of 99.999+% copper and zinc were prepared for this study.

A torsion loading system was developed to apply single, short duration stress pulses to the specimens. This system generates a zero mode torsional wave front with a rise time of 2 μsec in a 1.25 cm diameter elastic rod. The loading wave front, after passing through a specimen crystal, is reflected at a free surface normal to the cylindrical axis. The reflected wave unloads the specimen, and the duration of the stress pulse at any point is just the round trip travel time of the wave front from that point to the free surface. The torsion strain on the cylindrical surface of the elastic rod is monitored using semiconductor strain gages. The stress on a cross section of the specimen crystal varies linearly from zero on the cylindrical axis to a maximum at the surface. Dislocations were observed before and after stressing.

Copper cylinders with [100] axes, and 4, 3mm wide flats on {100} surfaces were tested at room temperature. Dislocation displacements up to 100μ into regions initially free of dislocations were measured on the {100} flats using the double etch technique. The dislocations were of mixed edge-screw orientation. The behavior of fresh dislocations produced by scratching and of isolated aged dislocations was not significantly different. The displacement was found to be a linear function of distance from the free end, therefore, the displacement was linearly proportional to the time of stress application. A nearly linear relationship between dislocation velocity and stress was found, stresses from 2.8 Mdyne/cm^2 to 23.1 Mdyne/cm^2 produced velocities from 160 cm/sec to 710 cm/sec.

---

* This work was sponsored by the United States Atomic Energy Commission under Contract No. AT(04-3)-473

Zinc crystals with a [0001] cylindrical axis and (0001) end surfaces were used to study basal dislocation mobility at room temperature. One end surface was scratched prior to stressing to produce fresh edge dislocations. The end surfaces were then bonded to elastic rods and a torsion pulse was applied. The bond on the scratched end of the crystal was removed, and displacement of dislocations from the scratches was observed using the Berg-Barrett X-ray diffraction technique. Dislocation displacement was found to be directly proportional to radial position from the cylindrical axis, which implies that the basal dislocation velocity is directly proportional to stress. Dislocation displacements up to approximately 400μ were measured. Interaction between different basal dislocations in these tests was negligible. The maximum test stress of 17.2 Mdynes/cm^2 produced a dislocation velocity of approximately 600 cm/sec. The mobility of basal dislocations in zinc was considerably reduced by aging for eight hours after scratching. This is attributed to the accumulation of jogs along the dislocations which were within 5μ of the observation surface.

These results indicate that the dislocation drag in copper and the basal system in zinc is relatively small compared to that in other materials in which direct observations have been made. The drag agrees well with that predicted for phonon interaction with the moving dislocations, and with the value deduced from internal friction measurements in copper. Tests are in progress to see if the dislocation velocity increases as the phonon interaction is reduced at lower temperatures.

Slip on the $\{1\bar{2}12\}\ \langle 1\bar{2}1\bar{3}\rangle$ system of zinc occurs by the formation and growth of slip bands. A dislocation etch and the Berg-Barrett technique were used to observe the growth of the slip bands produced by compression pulse loading of specimens in the [0001] and $\langle\bar{1}2\bar{1}0\rangle$ directions. The majority of slip bands are nucleated at substructure boundaries, and the bands grow at essentially equal rates in all directions on the $\{1\bar{2}12\}$ slip planes. Dislocation velocity at room temperature was found to be proportional to stress to the 8.7th power. The velocity at a given stress decreases with a decrease in temperature, and also decreases as the initial dislocation density increases. This indicates that motion of $\{1\bar{2}12\}\ \langle 1\bar{2}1\bar{3}\rangle$ dislocations is assisted by thermal activation and that forrest dislocations may be the most significant obstacles to their motion. Quantitative studies of the temperature and stress dependence are underway.

Dislocation Velocity in Copper and Zinc*

T. Vreeland, Jr.

W. M. Keck Laboratory of Engineering Materials

California Institute of Technology, U. S. A.

ABSTRACT

The stress dependence of dislocation velocity in copper and in the basal and 2nd order pyramidal slip systems of zinc has been measured. Dislocations were observed by the etch pit and Berg-Barrett x-ray techniques before and after application of short duration stress pulses. The velocity of dislocations of mixed edge-screw orientation in copper and of basal edge dislocations in zinc was found to be a linear function of stress at room temperature. This data gives a value of the dislocation damping constant of 7×10^{-4} dyne sec cm^{-2}, in good agreement with the value deduced from internal friction measurements in copper. Evidence of an unusual stress and temperature dependence for the velocity of dislocations in slip bands on the 2nd order pyramidal slip system of zinc is reported.

---

* This work was sponsored by the U. S. Atomic Energy Commission

INTRODUCTION

The stress-strain behavior of the F. C. C. metals is relatively insensitive to strain rate as compared, for example to that of the B. C. C. metals. Thus, the inverse strain rate sensitivity of the flow stress $\frac{\partial \ell n\ \dot{\epsilon}}{\partial \ell n\ \tau}$ is relatively large in the F. C. C. metals. This has been taken as an indication that the dislocation velocity is a sensitive function of stress in these metals, i.e. that the mobility exponent $\frac{\partial \ell n\ v}{\partial \ell n\ \tau}$ is relatively large[1].

Adams et al.[2] measured the inverse strain rate sensitivity of the flow stress in the basal system of zinc and found it was also relatively large. Measurements of the velocity of basal slip band growth in zinc[2] indicated that $\frac{\partial \ell n\ v}{\partial \ell n\ \tau}$ was significantly smaller than $\frac{\partial \ell n\ \dot{\epsilon}}{\partial \ell n\ \tau}$. However, an abrupt increase in velocity was found at about 0.5 Mdyne/cm^2, the velocity increasing from 0 to about 10 cm/sec. It was proposed that the abrupt increase in dislocation velocity occurs when attractive junctions between the basal and non-basal dislocations are broken. This, in effect, gives rise to a very large mobility exponent at the break-away stress, with a significantly smaller mobility exponent at higher stresses. The strain rate sensitivity of the flow stress appears to be influenced more by the large mobility exponent associated with the break-away process than with the smaller mobility exponent found at higher stresses. This phenomenon can be described in terms of a change in mobility exponent with stress, or in terms of a change in the density of mobile dislocations

with stress. The mechanism which limits the dislocation velocity in zinc at stresses in excess of 0.5 Mdyne/cm^2 was not established, but phonon drag was considered likely because of the relatively high velocities and low stresses.

Dislocations in the F. C. C. metals might behave in a similar manner. A discontinuous velocity vs stress relationship could exist for dislocations which have to cut through the forrest, the velocity increasing from zero to a high value at the break-away stress. This could account for the very small strain rate sensitivity. Further, the stress sensitivity of dislocation velocity at stresses above the yield stress could be relatively small. The investigations reported here were undertaken to explore this possibility, and to gain further information on the stress dependence of dislocation velocity in zinc.

Direct measurements of dislocation displacements in copper and in the basal system of zinc were made. The displacements were produced by short duration, essentially square pulse loading, and dislocation velocities were calculated from the observed displacement and pulse length. Dislocation-dislocation interactions were minimized in these experiments, and the drag force on moving edge-screw dislocations in copper and basal edge dislocations in zinc was determined.

The torsional loading system devised to limit the displacement of high velocity dislocations to distances small compared to the initial dislocation spacing (in crystals of good quality) is first described. Torsional loading of copper and etch pit observations on (100) surfaces, and torsional loading on zinc with Berg-Barrett x-ray observations of (0001) surfaces is then described. These observations are discussed

and contrasted to the behavior of dislocations in other materials.

VELOCITY MEASUREMENTS

Torsional Loading System

Single torsional stress pulses of microsecond duration were applied to the specimens by means of the machine described by Pope et al.[3]. This machine utilizes zero-order mode torsional waves in cylindrical bars which are generated in the following manner. An initial static torque is applied to a section of a cylindrical rod which is a part of the torsion rod system shown schematically in Fig. 1. The torque is applied to the top of the section by dead weight loading of a cranking disc attached to the rod through a rubber sleeve. A 0.015 cm thick glass disc cemented to the bottom of the section transmits this torque to a bakelite fixture which is attached to a fixed bearing tube surrounding the rod. A 0.005 cm thick aluminum foil is cemented between the glass disc and bakelite with Eastman 910 adhesive. The lower section of the torsion rod is attached to the opposite side of the glass disc by means of a butt adhesive bond. This section of the torsion rod is coaxial with the upper section but does not carry any static torque. The specimen assembly is attached to the bottom end of this lower section of the torsion rod, and the bottom end of the specimen assembly is the free end of the torsion rod system. The section of the rod above the cranking disc (damping section) is coated with a viscoelastic material in order to attenuate the waves propagating away from the specimen.

The application of the stress pulse to the specimen is initiated by a high-voltage capacitor discharge through the aluminum foil. Explosion

of the foil releases the static torque and results in elastic waves which propagate away from the glass disc interface of the torsion rod. The amplitude of the dynamic torque in the lower section of the torsion rod is one-half the initial static torque applied to the machine, and therefore, proportional to the weight hung on the cranking disc. The duration of the stress pulse at any point in the specimen is the time required for the wave to propagate from that point to the free end and return.

The stress wave generated by the release of the static torque propagates without dispersion through the isotropic elastic rod attached to the glass disc because the elastic zero-order mode torsional waves are non-dispersive. The propagation of zero-order mode torsional waves in ⟨100⟩ axis copper specimens and in [0001] axis zinc specimens is also non-dispersive and the distribution of shear stress over a cross-section of a specimen is the same as that in an isotropic material.

The materials and dimensions of the rod system of the torsion machine were chosen so as to make the acoustic impedance of all the rod sections nearly equal to that of the specimen. Torsional wave reflections at the interfaces between different materials in the load train were thereby minimized. Steel rods of 1.27 cm diameter were used in the tests on copper and titanium rods of the same diameter were used in the tests on zinc. A thermal buffer of polycrystalline copper was cemented between the steel rod and the copper specimen. A monel thermal buffer was used in the zinc tests. The buffers prevented spurious thermal stresses in the specimens because the differential expansion of the specimen and buffer was negligible. All sections of the specimen-torsion rod system were joined together by means of Eastman 910 adhesive for the copper tests.

A special bonding technique was devised to join the monel to the zinc so that dislocations were not displaced when the bond was made or when it was removed. This technique is described in a following section.

The amplitude and duration of the stress pulse were measured by means of silicon strain-gages, cemented to the torsion rod. The strain-gage output was displayed on a dual beam oscilloscope. The upper beam was triggered by the capacitor discharge employed to initiate the torsion wave and had a sweep rate of 200 μsec/cm. This provided information about any reflected stress pulses applied to the specimen at relatively long times after the primary stress pulse. The initiation of the lower trace was appropriately delayed and its sweep rate was 20 μsec/cm. The lower trace provided detailed information regarding the primary stress pulse. A record of strain gage output vs time with no specimen attached to the titanium elastic rod system is shown in Fig. 2. The gages were located 19.5 cm from the free end of the rod system for this record, and the pulse length is just the time required from elastic shear wave in titanium to travel from the gage to the free end and return.

The dislocation displacements in the specimen crystals which are induced by the stress pulse must give rise to plastic strains which are small compared to the elastic strains associated with the pulse if dispersion is to be avoided. Thus, only a low density of moving dislocations can be tolerated when the dislocation velocity is large.

Testing of Copper Crystals

Experiments were performed on single crystal copper specimens in the form of right circular cylinders 1.25 cm in diameter. The cylindrical

axis was parallel to the [100] crystal axis to within $\pm \frac{1}{2}^{\circ}$. The cylindrical surface was modified by four flat {100} observation surfaces, each about 0.3 cm wide, spaced at 90° intervals around the circumference and extending the full length of the specimen.

These test specimens were machined from larger single crystals. The crystals were grown in graphite crucibles from a charge of 99.999% copper by the modified Bridgman technique employed by Young and Savage[4]. Rough machining of specimens was performed by trepanning and wire slicing using spark erosion machines. Finish machining was accomplished by chemical lapping using a saturated solution of cupric chloride in concentrated hydrochloric acid and a rotating cloth-covered Lucite wheel. At least 0.04 cm thickness of material was removed by chemical lapping, thus removing the mechanical surface damage due to spark erosion machining. The test specimens were annealed for about 100h at 1030 ± 10°C in a hydrogen atmosphere after finish machining.

Fresh dislocations were introduced into specimens by scratching the {100} observation surfaces in a controlled manner with a diamond phonograph stylus or an alumina whisker by means of a special scratching apparatus. Scratching was performed after the surface had been chemically polished in the manner employed by Livingston[5].

Specimens were etched prior to stress application either by the solution used by Livingston[5] or by that used by Young[6]. The etch revealed grown in dislocations on the {100} observation surfaces and the fresh dislocations produced by scratching. A permanent record of this dislocation configuration was obtained by making a replica of the specimen surface on a cellulose acetate film.

Four tests were performed with nominal resolved shear stresses at the outer radius of the specimen ranging from 2.5 to 25 M dyne/cm^2. A different specimen was used in each test.

Analysis of the stress pulse records shows that the major portion of the torsional wave in the specimen propagated in an elastic manner. Thus, to a first approximation, the magnitude of the stress is independent of position along the specimen and the duration of stress is linearly proportional to distance from the free end of the specimen.

The stress vs time relation at the loaded end of the specimen may be determined from the test record even when plastic wave propagation takes place. This is because both the indicent and reflected waves which propagate between the strain gages and the loaded end of the specimen are purely elastic and propagate at known wave velocities. The actual stress pulse shape at the loaded end for each test was determined from the four records. The pulses were trapazoidal, rather than square. The dislocation displacement corresponding to the loaded end of the specimen was found by extrapolation of measurements of displacement vs distance from the free end as explained below.

The specimen was re-etched and the observation surfaces were replicated again immediately after testing. Photomicrographs of the replicas of specimen number 3-3-1 taken before (a) and after (b) the application of the stress pulse are shown in Fig. 3. The scratch (horizontal in the photomicrographs) is parallel to the cylindrical axis of the specimen. The replicas were carefully examined to find the original and final positions of individual dislocations. The distance between the original and final positions of these dislocations was

measured to within ± 4 microns.

The dislocation lines extending into the interior of the test specimen from the observed etch pits are probably oriented nearly at right angles to the trace of the {111} slip planes on the {100} observation surface. A pure edge dislocation so oriented has zero resolved shear stress applied to it. The dislocations which moved were therefore presumed to be of mixed edge-screw orientation.

Mean values of measured dislocation displacement are plotted as a function of distance from the free end of the specimen in Fig. 4 for the four tests conducted. The number of individual dislocation displacements measured is indicated near each plotted point. The vertical lines through the plotted points represent the standard deviation of the measurements. The maximum standard deviation is 13% of the mean dislocation displacement. The straight lines in Fig. 4 were drawn to represent the data. This shows that the dislocation displacement is linearly proportional to distance from the free end of the specimen. The points marked "x" at the end of each line in Fig. 4 represent the extrapolated value of dislocation displacement at the loaded end of each specimen.

The observed linear relationship between dislocation displacement and distance from the free end of the specimen is consistent with the assumptions that the stress wave propagates through the specimen in an elastic manner and that the acceleration time for the dislocations is negligible. If we assume a square, rather than a trapazoidal pulse, the duration of stress, Δt, is related to distance from the free end of the specimen, x, by

$$\Delta t = 2\frac{x}{c} \quad , \tag{1}$$

where $c = 0.290 \times 10^6$ cm/sec is the velocity of propagation of an elastic torsional wave along the ⟨100⟩ specimen axis. Thus, if Eq. 1 is employed to convert the abscissa scale of Fig. 4 to a scale of time duration of stress, the slopes of the lines are equal to the dislocation velocity. First approximation values of dislocation velocity, v, determined in this manner are found to be approximately proportional to the m = 0.7 power of the resolved shear, τ, when these data are fitted to an equation of the form

$$v = v_o \left(\frac{\tau}{\tau_o} \right)^m \tag{2}$$

where m and τ_o are material constants and v_o is unit velocity. This result indicates, however, that a significant portion of the total dislocation displacement occured during the rising and falling portions of the trapazoidal stress pulses. For this reason a more refined method of analysis of the experimental measurements was employed which used the actual stress pulses shape to determine corrected values of dislocation velocity as a function of resolved shear stress.

When the corrected values of dislocation velocity vs stress are fit to a power law functional relationship, the "best fit" is still obtained by employing a stress exponent, m = 0.7. The "fit" is not quite as good if it is assumed that the exponent is m = 1. However, the scatter and uncertainty in the experimental measurements are such that the value m = 1 may be the true value. Thus, the resistance to the motion of

individual dislocations in 99.999% pure copper may be described approximately as a simple linear viscosity, at least in the dislocation velocity range of 100 to 1000 cm/sec. A plot of the corrected dislocation velocity vs the resolved shear stress is given in Fig. 5. The solid line is given by the equation

$$v = v_o \left(\frac{\tau}{2.7 \times 10^4} \right) \tag{3}$$

with v_o = 1 cm/sec and τ in dynes/cm^2.

Testing of Zinc Crystals

Torsion pulse tests were made on three [0001] axis zinc crystals. The specimen assembly which was used is shown in Fig. 6. Strain gages were placed 0.15 cm from the monel-specimen interface, and titanium rods were bonded to the other end of the specimen to obtain the desired stress pulse duration.

Prior to torsion pulse loading, edge dislocations were generated near the (0001) surface which was to be bonded to the monel thermal buffer. The dislocations were generated by scratching the surface using an Al_2O_3 whisker and a 50 mg load. When the scratch direction is perpendicular to a $\langle 11\bar{2}0 \rangle$ slip vector, parallel edge dislocations of the same sign move out from the scratch and are revealed in a Berg-Barrett photograph. The technique employed by Armstrong and Schultz[7] was used to obtain the Berg-Barrett photographs shown in Fig. 7. Basal dislocations which lie within about 5μ of the surface are revealed in these photographs. The dislocations parallel to the three scratch segments shown in the

$(01\bar{1}3)$ reflection are extinct in the (0004) and $(10\bar{1}3)$ reflections so they must have a Burgers vector in the $[1\bar{2}10]$ direction. Specimens were scratched along three diameters of an (0001) end surface, the scratches were made in short segments and were perpendicular to a $\langle 1\bar{2}10 \rangle$ direction. The scratched surface was then bonded to a monel thermal buffer, and a stress pulse was applied.

The bonding was found to be a very critical operation because conventional techniques produced sufficient shear stress to move the fresh dislocations generated by the scratch. Phenyl salicilate (salol), an organic crystalline material, was found to be a satisfactory bonding agent. It readily supercools to room temperature but undergoes a large volume change when it solidifies. The large volume change does not cause difficulties if the specimen surface is coated with a seed layer of salol (by spraying it with an artists air brush). The seeded surface is then brought into contact with the monel rod which has a layer of supercooled salol on its surface. The salol bond is readily dissolved in acetone, and a comparison of Berg-Barrett photographs taken before bonding and after dissolving the bond showed only minor changes in dislocation positions (<0.002cm).

Specimens were bonded and tested immediately after scratching. The bond was then dissolved, and Berg-Barrett photographs were taken. A Berg-Barrett photograph was not taken after scratching as it was found that the fresh dislocations became relatively immobile with aging.

Berg-Barrett photographs of the dislocation arrangement around three scratch segments on an untested and on a tested specimen are shown in Fig. 8. Dislocation motion took place in the direction of the applied

shear stress, and varied with radial position on the (0001) surface.

Measurements of the maximum dislocation displacement from each scratch segment were made. They are plotted in Fig. 9 as a function of radial position. These displacements are the sum of the displacement due to scratching and that due to the stress pulse. The displacement due to scratching was taken as the intercept of the line (least squares fit) through the experimental points. This displacement was subtracted from the measured displacement to obtain the displacement which was produced by the stress pulse.

The plastic strain in the specimens was small compared to the elastic strain produced by the stress pulse. This can be shown by consideration of the dislocation displacements observed and the known density of basal dislocations in the bulk of the crystals (approximately 10^4 cm^{-2}). Therefore, the stress distribution was that associated with the elastic waves, namely a stress which varies linearly with radius. The maximum stress occurs at the outer radius of the specimen and this stress was deduced from the strain gage signal. The stress pulse shape was essentially square, and its duration was independent of radial position at the monel buffer-specimen interface.

Since both stress and dislocation displacement were linear functions of radial position, dislocation velocity is a linear function of applied shear stress. The velocity corresponding to each displacement measurement was calculated (taking into account the small deviations from a square stress pulse) and the results are given in Fig. 10 as a function of stress. The data in Fig. 10 are fitted with the straight line

$$v = v_o \left(\frac{\tau}{2.94 \times 10^4} \right) \qquad (4)$$

with v_o = 1 cm/sec and τ in dynes/cm^2. The scatter in the velocity vs stress data is greater than experimental uncertainties in the measurements of stress (± 10%), dislocation displacement (± 2 x 10^{-3} cm), and time (± 5%). Sources of this scatter are considered below.

The line tension of a curved dislocation could modify the net force on the dislocation. A typical radius of curvature of the dislocations on a tested specimen is 0.018 cm. The stress required to maintain this radius (0.5 Mdynes/cm^2) is small compared to the stresses applied to the dislocations whose displacements were measured.

The final spacing of basal dislocations which moved from the scratch was sufficiently large that their interaction stresses were negligible compared to the applied stress. It was concluded that they were spaced widely enough during most of their motion so that interaction forces between them can be neglected. Interaction of the basal dislocations with forrest dislocations was probable. The forrest density ranges between 10^3 and 10^4 cm^{-2} in the zinc crystals tested, so that moving basal dislocations intersected forrest dislocations every 0.02 cm on the average. Since basal dislocation displacements measured in this work varied from about 0.01 to 0.04 cm, interaction with forrest dislocations could be responsible for much of the observed scatter.

The effect of drag due to point defects cannot be assessed. Every attempt was made to minimize the number of point defects at the dislocations. High purity material was used (99.999+% zinc), and the aging time after scratching and before testing was held to a minimum.

DISCUSSION

The mixed screw-edge dislocations in copper and the basal edge dislocations in zinc have nearly the same linear velocity vs stress relationship. This velocity vs stress behavior is compared in Fig. 11 to that in some other materials on which direct measurements have been made. The copper and zinc measurements are unique in that they exhibit the highest velocities in the low stress range. This indicates relatively weak interactions between the moving dislocations and other lattice defects. In fact, the majority of dislocation drag in the tests on copper and zinc may have been due to phonon interaction.

A comparison of the direct dislocation drag measurements reported here, and the drag deduced from internal friction measurements in copper is given in Table 1. The damping constant derived from the results of this study, $B = b\tau_o/v_o$ in the notation used here, is in good agreement with the room temperature measurements of Alers and Thompson[12] and Stern and Granato[13]. Tests are in progress to see if B is reduced at lower temperatures as predicted by the phonon interaction theories[15,16]. It is of interest to note that the dislocation displacements in the tests reported here were several orders of magnitude greater than the displacements in the internal friction experiments.

The small rate sensitivity of the flow stress in copper and in basal slip in zinc may be attributed to a strong stress dependence of the density of moving dislocations. Adams, et al.[2] suggested that a strong stress dependence of the moving dislocation density comes about when the internal stress amplitude is comparable in magnitude to the applied stress. The

average velocity of a dislocation in copper or zinc should be unaffected by the internal stress, provided that the displacement is large compared to the wave length of internal stress fluctuations and the total stress does not drop to zero. This is a consequence of the linear relation between stress and velocity and the fact that the average stress on the slip plane is equal to the applied resolved shear stress. When the internal stress amplitude is comparable in magnitude to the applied stress, dislocations will be trapped wherever the total stress drops to zero, and very small changes in the applied stress can change the velocity of a significant number of dislocations from zero to the relatively high value corresponding to the applied stress. The rate sensitivity of the flow stress is thereby very small.

The velocity of dislocations on the 2nd order pyramidal slip system on zinc have a very unusual stress and temperature dependence. The experiments mentioned in the abstract have been extended to cover a range of temperatures, and the rather surprising results will be reported elsewhere. Briefly, the following observations have been made on dislocations in slip bands on the $\{1\bar{2}12\}\ \langle 1\bar{2}1\bar{3}\rangle$ slip system in high purity, acid machined crystals.

1. At temperatures below 110°K the mobility exponent is relatively low, (1.7), thermally activated motion seems probable with an activation volume $\approx 6b^3$ and an activation energy of 1/4 eV. Screw dislocations in slip bands exhibit velocities approximately 5X higher than edge dislocations.

2. A more complex mechanism of dislocation motion is indicated at temperatures above 110°K. The mobility exponent increases rapidly with

temperature above 250°K and the ratio of screw to edge velocity is unity above 250°K.

3. The stress required to maintain a given dislocation velocity goes through a minimum as the temperature is varied between 77°K and 320°K.

TABLE 1

DISLOCATION DAMPING CONSTANT IN COPPER AT ROOM TEMPERATURE, 10^{-4} dyne sec/cm^2

This study	7
Alers and Thompson[12]	8
Stern and Granato[13]	6.5
Suzuki, et al.[14]	0.79

ACKNOWLEDGEMENTS

The experiments on copper reported here were conducted by my former student W. F. Greenman, now on a post-doctoral Fullbright Fellowship at the Max Planck Institute, Stuttgart. The experiments on basal slip in zinc were conducted by my former student D. P. Pope, now a research fellow at the W. M. Keck Laboratory of Engineering Materials. The interesting results on 2nd order pyramidal slip were obtained by Mr. R. C. Blish as part of his thesis research. Stimulating discussions with these students and with Mr. A. P. L. Turner who contributed greatly to our ability to effectively use the Berg-Barrett technique are gratefully acknowledged. The patient counsel of my colleague, Professor D. S. Wood, throughout this work is sincerely appreciated. Mr. G. R. May gave valuable assistance in the growth of crystals and the preparation of test specimens.

REFERENCES

1. A. H. Cottrell, The Relation between the Structure and Mechanical Properties of Metals, Vol II (London: Her Majesty's Stationery Office, 1963), pp. 456.
2. K. H. Adams, T. Vreeland, Jr., and D. S. Wood, Materials Eng. and Sci, in press.
3. D. P. Pope, T. Vreeland, Jr., and D. S. Wood, Rev. Sci. Instr. 35 1351 (1964).
4. F. W. Young, Jr., and J. R. Savage, J. Appl. Phys. 35, 1917 (1964).
5. J. D. Livingston, J. Aust. Inst. Metals. 8, 15 (1963).
6. F. W. Young, Jr., J. Appl. Phys. 32, 192 (1961).
7. J. M. Schultz and R. W. Armstrong, Phil. Mag. 10, 497 (1964).
8. W. G. Johnston and J. J. Gilman, J. Appl. Phys. 30, 129 (1959).
9. D. F. Stein and J. R. Low, Jr., J. Appl. Phys. 31, 362 (1960).
10. E. Yu. Gutmanas, E. M. Nadgornyi, and A. V. Stepanov, Soviet Phys. Solid State 5, 743 (1963).
11. H. W. Schadler, Acta Met. 12, 861 (1964).
12. G. A. Alers and D. O. Thompson, J. Appl. Phys. 32 283 (1961).
13. R. M. Stern and A. V. Granato, Acta Met. 10, 358 (1962).
14. T. Suzuki, A. Ikushima, and M. Aoki, Acta Met. 12, 1231 (1964).
15. G. Leibfried, Z. Physik. 127, 344 (1950).
16. W. P. Mason, J. Acoust. Soc. Am. 32, 458 (1960).

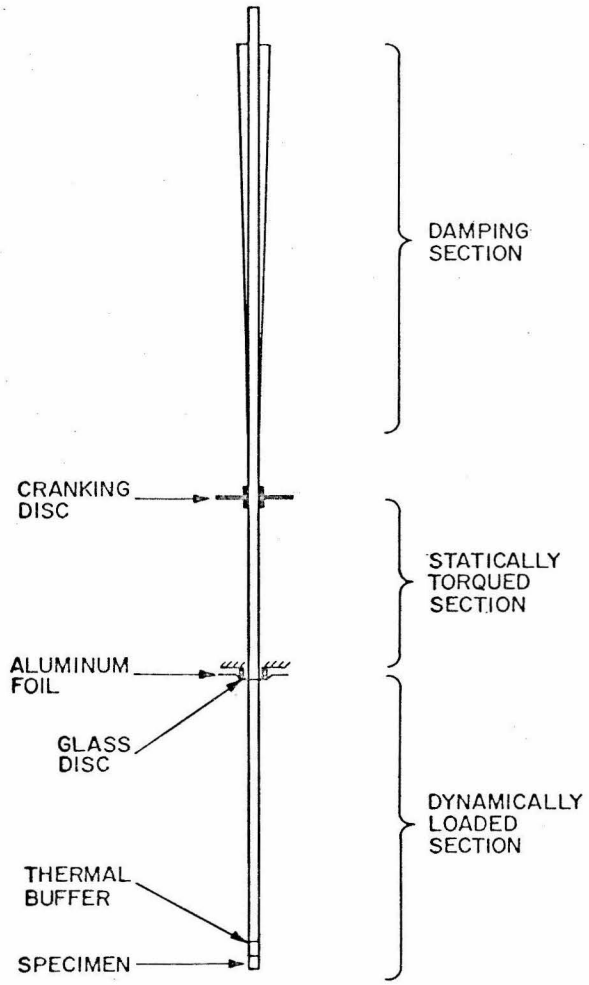

Fig. 1 Schematic of Torsion Pulse System

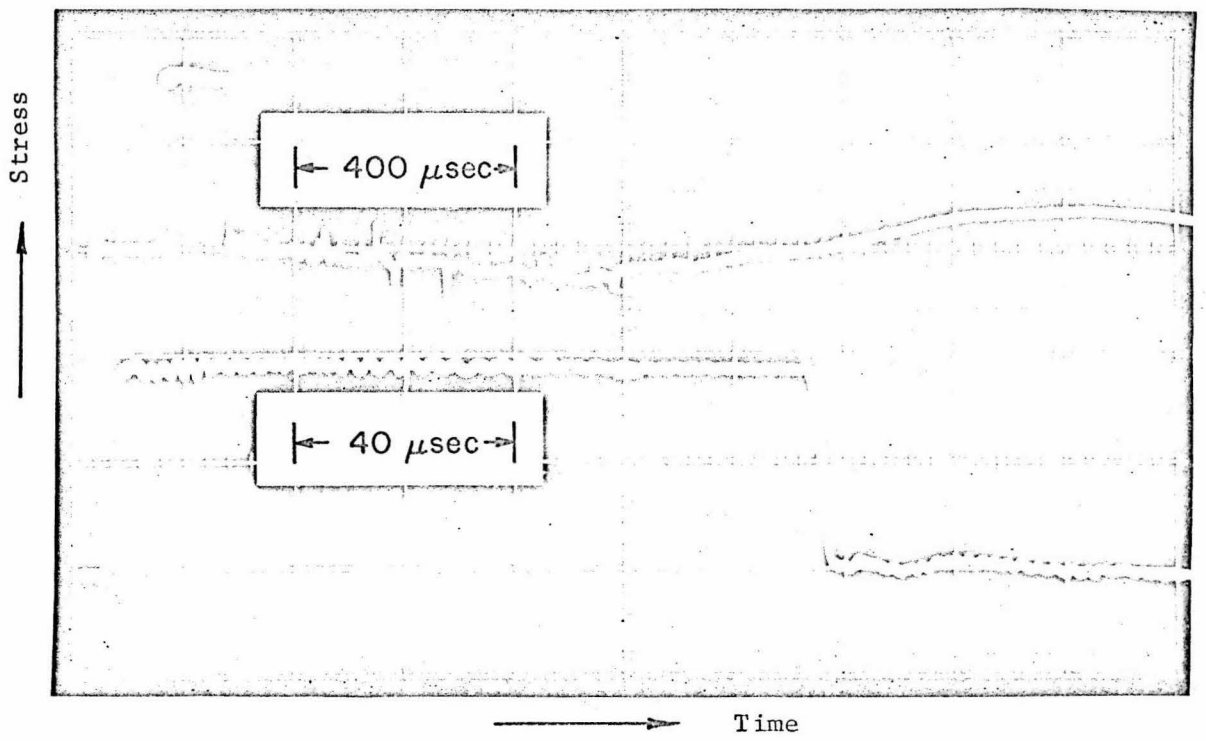

Fig. 2 A Stress Pulse Produced by the Torsion Loading System

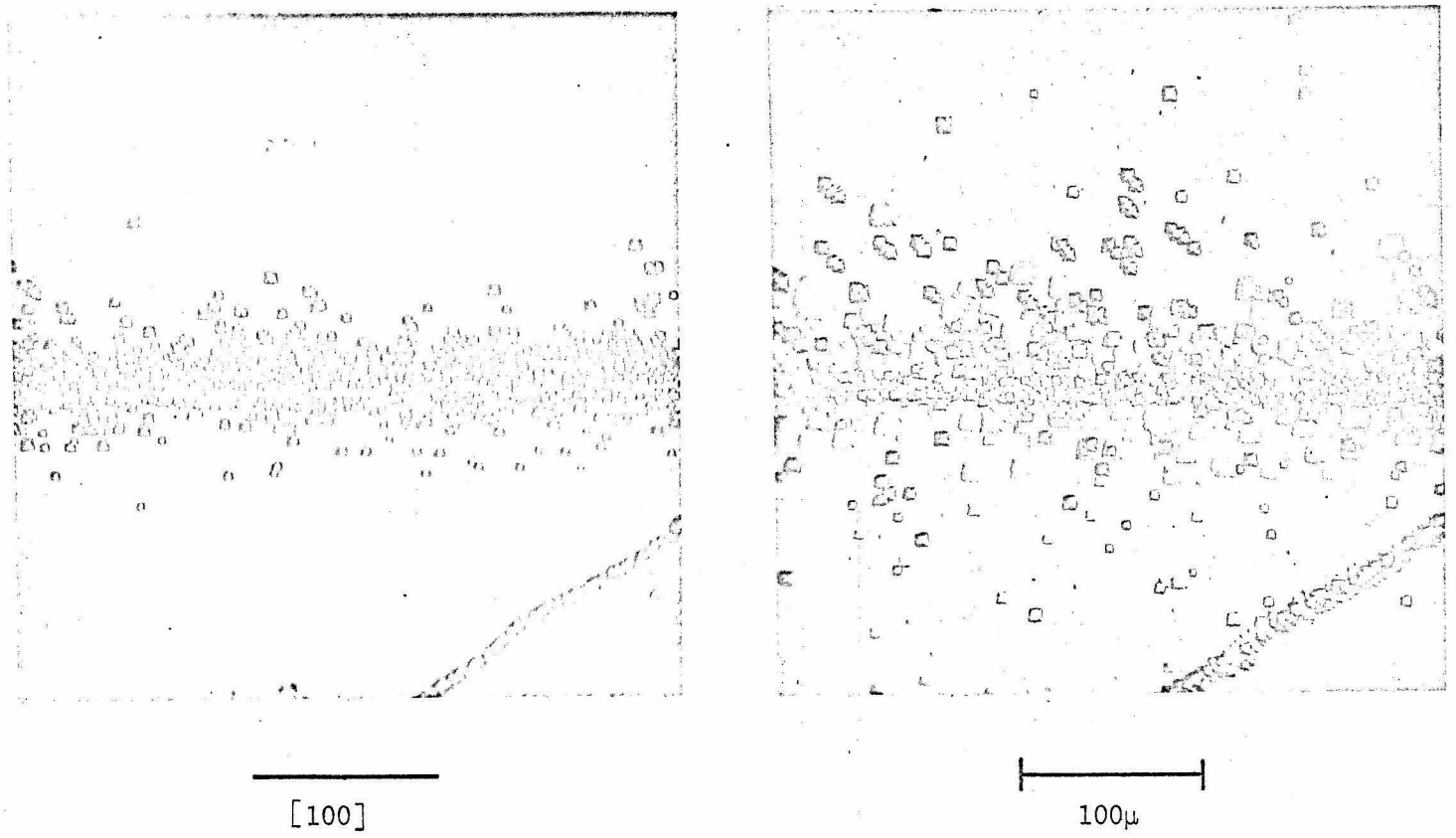

Fig. 3 Etch Pits Near a Scratch on a Copper Specimen Before and After a Stress Pulse Was Applied

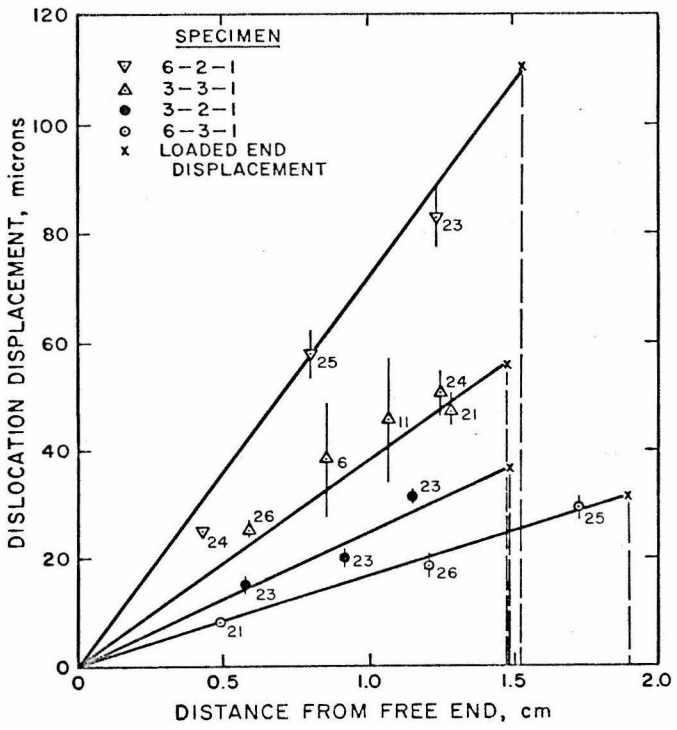

Fig. 4 Dislocation Displacement vs Distance from the Free End of Copper Specimens

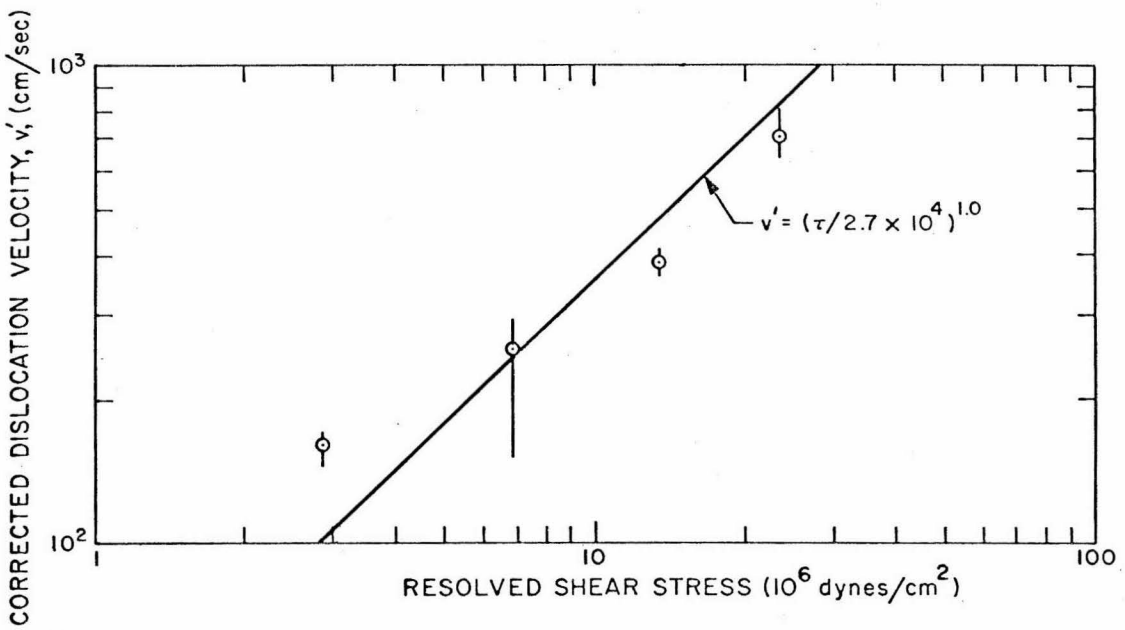

Fig. 5 Corrected Dislocation Velocity vs Resolved Shear Stress in Copper

Monel Zinc Titanium

Fig. 6 Zinc Specimen Bonded to Monel Strain Gage Rod and Titanium Extender

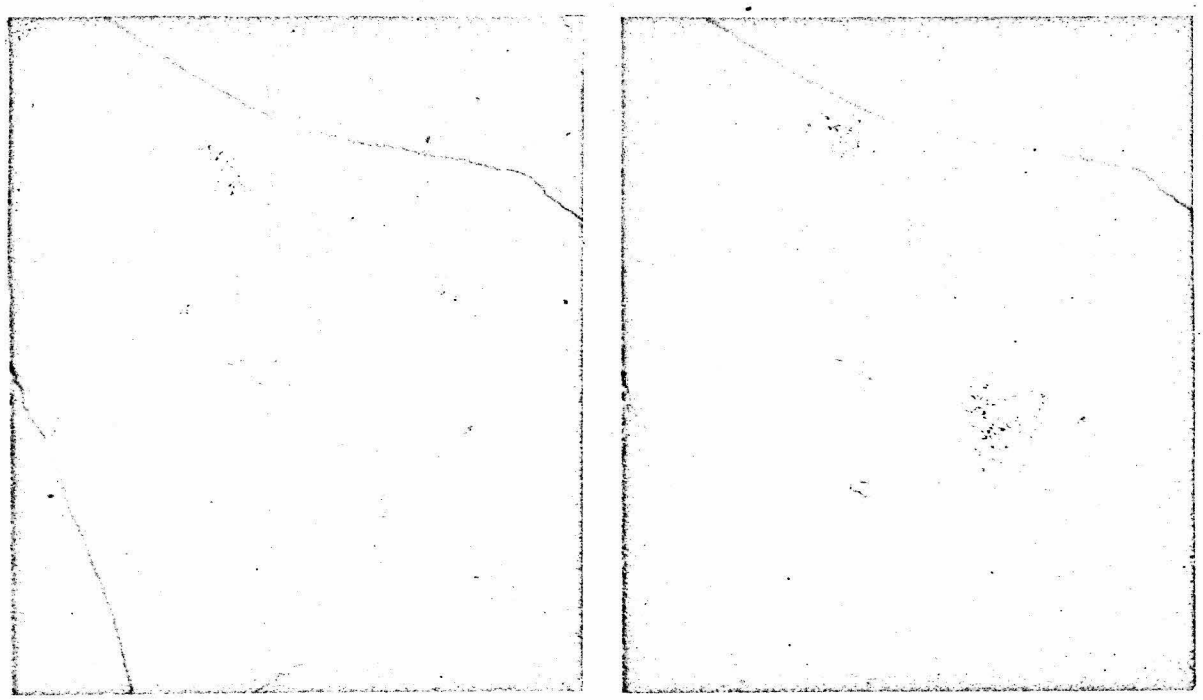

$(01\bar{1}3)$ Reflection $(10\bar{1}3)$ Reflection

$[1\bar{2}10]$ 0.04 cm

Fig. 7. Berg-Barrett Photographs of Scratched (0001) Surface of Zinc Using Two Different Reflecting Planes. Scratch is Along $[10\bar{1}0]$, Co Kα Radiation

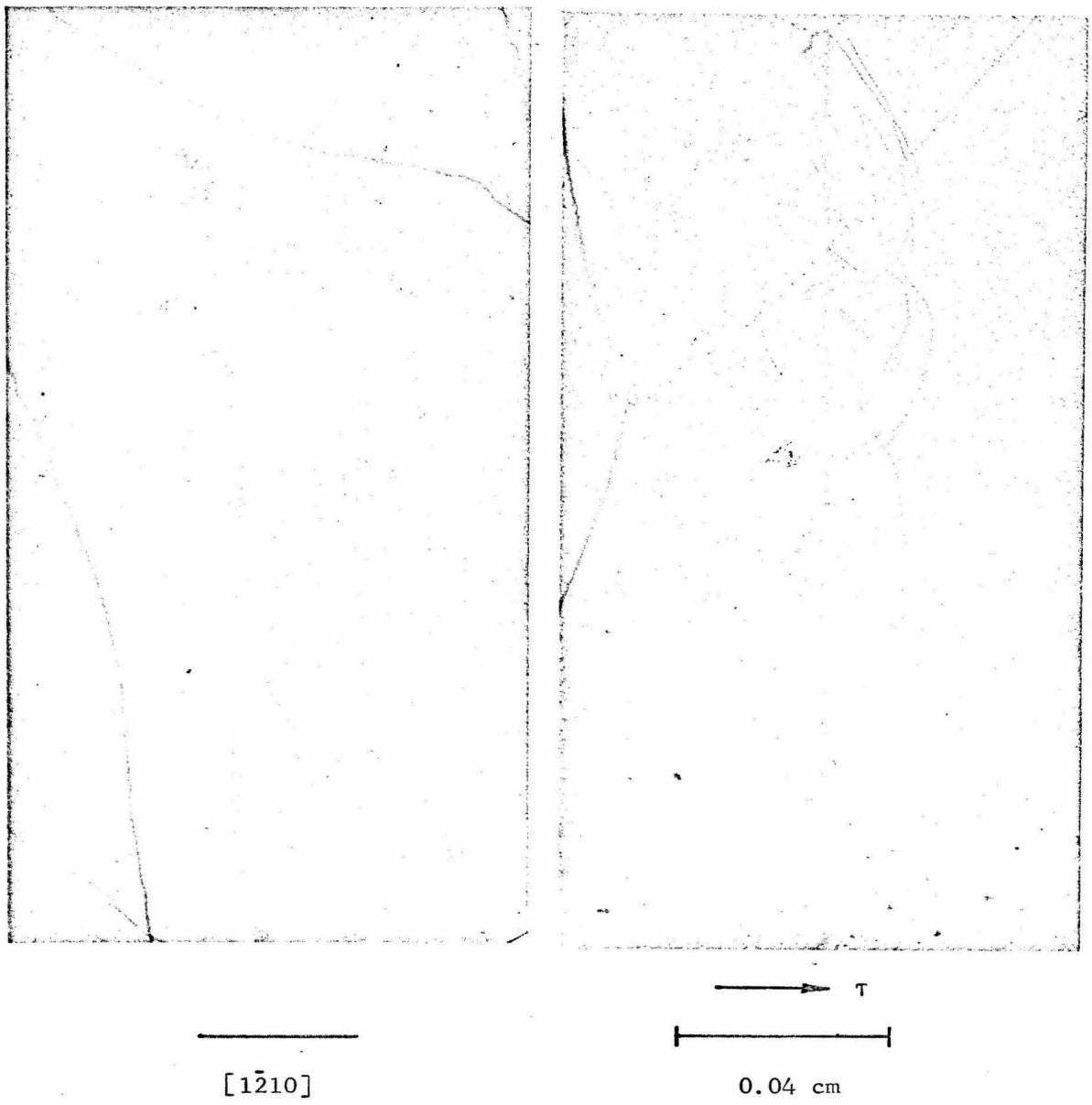

Fig. 8. Berg-Barrett Photographs of Dislocations Near a Scratch on an Untested and on a Tested Zinc Specimen (Different Specimens). Note Dislocation Displacements are in the Direction of the Applied Stress.

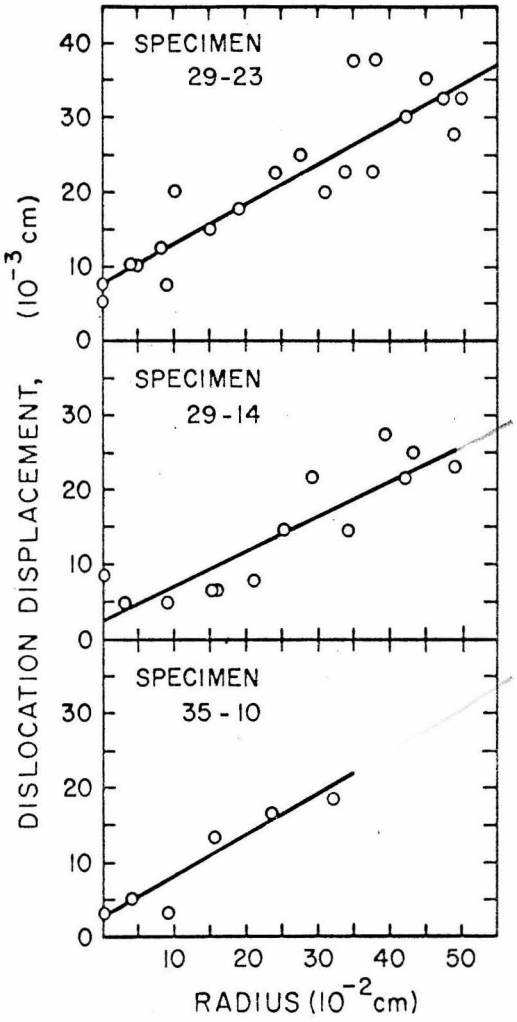

Fig. 9 Dislocation Displacement Plotted Against Radial Position on the Zinc Specimens

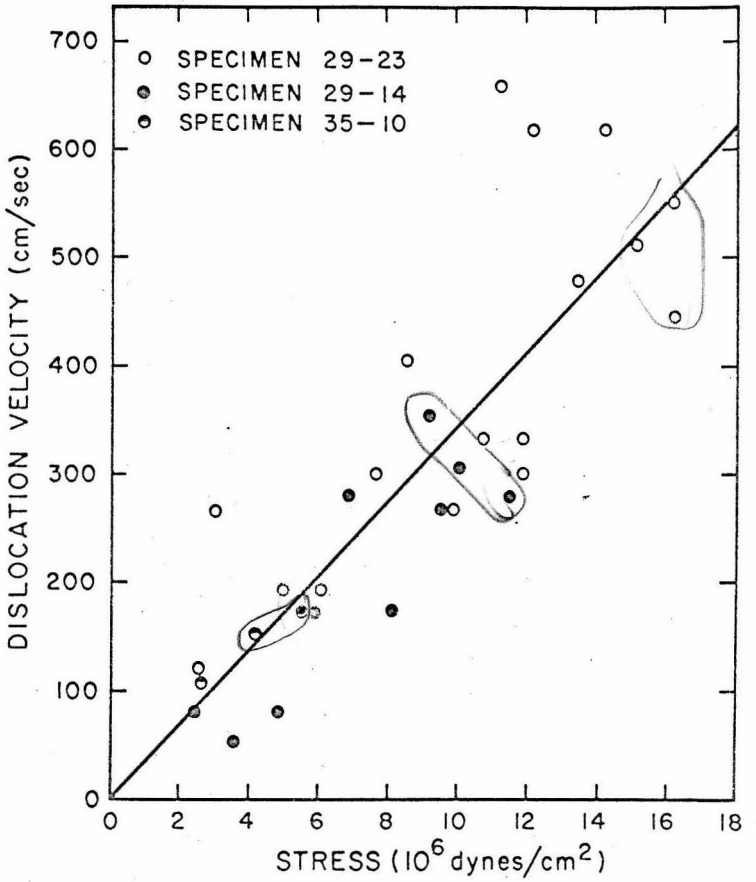

Fig. 10 Edge Dislocation Velocity in Zinc as a Function of Applied Resolved Stress

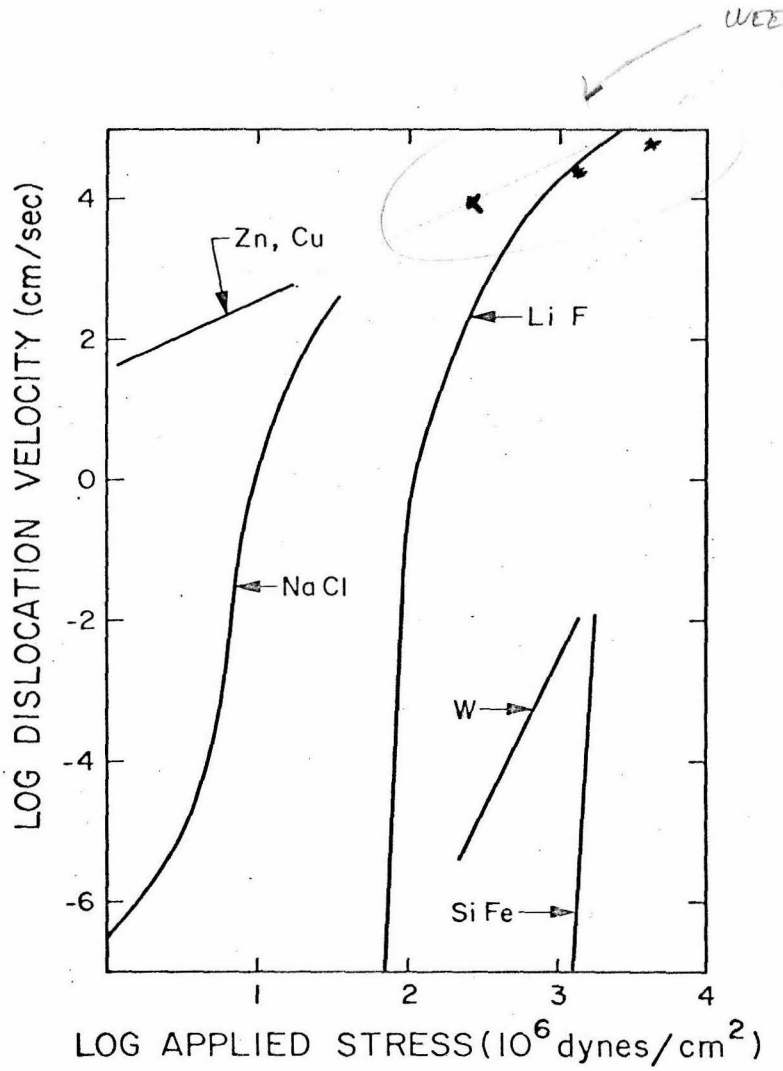

Fig. 11 A Comparison of the Velocity vs Stress Relationship in Cu, Zn, LiF[8], SiFe[9], NaCl[10], and W[11]